



# Synthesis, properties, and applications of topological quantum materials

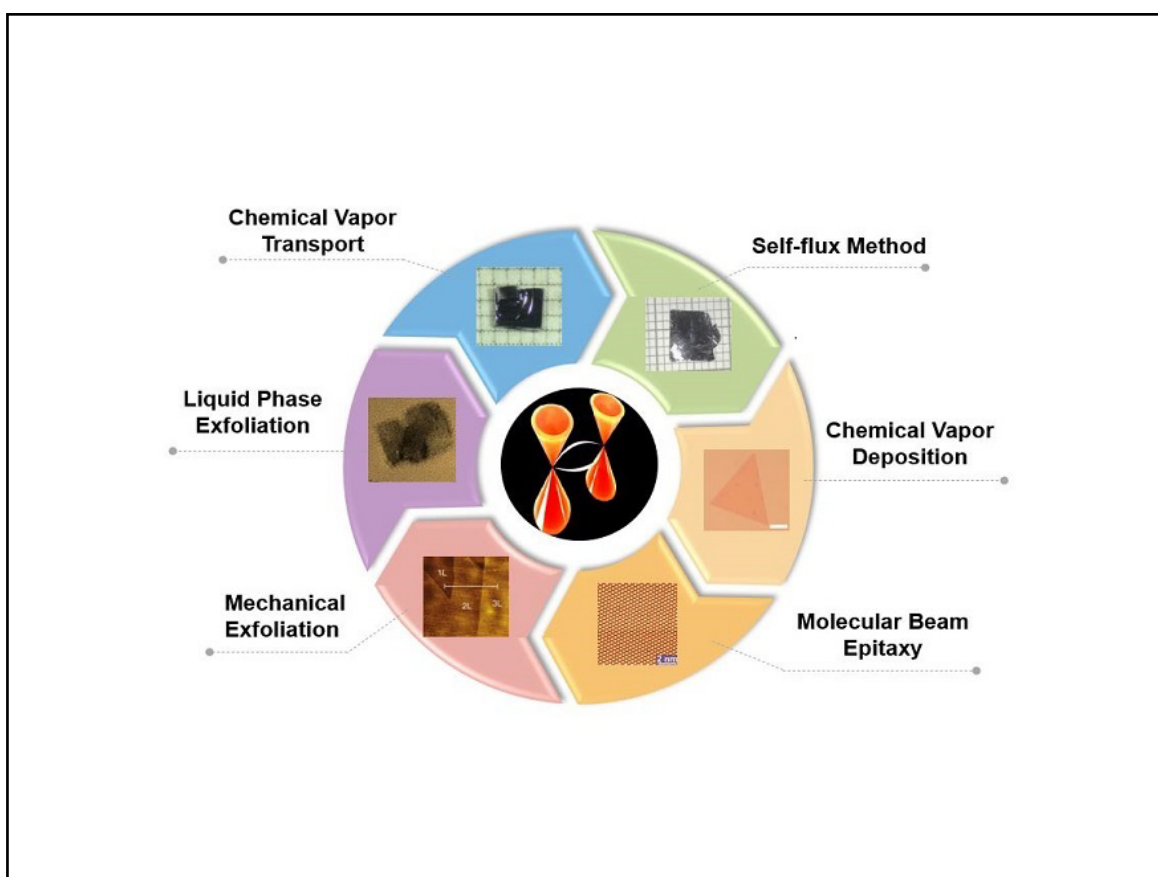
Junjie Wu, Ying Zhang, and Bin Xiang 

Department of Materials Science & Engineering, CAS Key Lab of Materials for Energy Conversion, Anhui Laboratory of Advanced Photon Science and Technology, University of Science and Technology of China, Hefei 230026, China

 Correspondence: Bin Xiang, E-mail: [binxiang@ustc.edu.cn](mailto:binxiang@ustc.edu.cn)

© 2023 The Author(s). This is an open access article under the CC BY-NC-ND 4.0 license (<http://creativecommons.org/licenses/by-nc-nd/4.0/>).

## Graphical abstract




*The typical synthesis of topological quantum materials.*

## Public summary

- The review presents the synthesis of two typical topological quantum materials.
- Topological magnets and topological superconductors with their potential physical properties and applications are discussed.
- Research related to the study of topological quantum material systems is of great importance.

# Synthesis, properties, and applications of topological quantum materials

Junjie Wu, Ying Zhang, and Bin Xiang 

*Department of Materials Science & Engineering, CAS Key Lab of Materials for Energy Conversion, Anhui Laboratory of Advanced Photon Science and Technology, University of Science and Technology of China, Hefei 230026, China*

 Correspondence: Bin Xiang, E-mail: [binxiang@ustc.edu.cn](mailto:binxiang@ustc.edu.cn)

© 2023 The Author(s). This is an open access article under the CC BY-NC-ND 4.0 license (<http://creativecommons.org/licenses/by-nc-nd/4.0/>).



Cite This: *JUSTC*, 2023, 53(10): 1002 (11pp)



Read Online

**Abstract:** Since topological quantum materials may possess interesting properties and promote the application of electronic devices, the search for new topological quantum materials has become the focus and frontier of condensed matter physics. Currently, it has been found that there are two interesting systems in topological quantum materials: topological superconducting materials and topological magnetic materials. Although research on these materials has made rapid progress, a systematic review of their synthesis, properties, and applications, particularly their synthesis, is still lacking. In this paper, we emphasize the experimental preparation of two typical topological quantum materials and then briefly introduce their potential physical properties and applications. Finally, we provide insights into current and future issues in the study of topological quantum material systems.

**Keywords:** synthesis; topological quantum materials

**CLC number:** O413; O469

**Document code:** A

## 1 Introduction

Condensed matter physics, which focuses on the motion patterns and laws of systems composed of a variety of particles, has become one of the most significant subdisciplines of physics. In 1980, the integer quantum Hall effect (IQHE) was discovered in experiments<sup>[1]</sup>, and more topological quantum states were found later<sup>[2]</sup>, indicating that the door to topological quantum materials is open to scientists all over the world. Since topological quantum materials may possess interesting properties and promote the application of electronic devices, the search for new topological quantum materials has become the focus and frontier of condensed matter physics.

It has been found that there are two interesting systems in topological quantum materials, topological superconducting materials and topological magnetic materials. Compared to traditional superconductors, topological superconductors have topologically protected metal states on the surface and superconducting states inside<sup>[3]</sup>. Furthermore, they possess an implacable excitation of quasiparticles, known as Majorana fermions<sup>[4,5]</sup>, on their boundaries, making them ideal materials for error-free quantum computers<sup>[6]</sup>. A topological magnet is a theoretical concept that intertwines magnetism and topology. Studies show that they are intensely influenced by the electronic wave functions and spin configuration. These materials have chiral edge states, which have a possible capability to realize low energy loss of electronic devices and have become another crucial system for studying topological quantum states<sup>[7-9]</sup>.

Although research on topological superconducting and topological magnetic materials has made rapid progress<sup>[10,11]</sup>, a

systematic review of their synthesis, properties, and applications, particularly their synthesis, is still lacking. Therefore, we emphasize the experimental preparation of two typical topological quantum materials and then briefly introduce their potential physical properties and applications to provide readers with an overview of topological quantum physics.

## 2 Synthesis of topological quantum materials

The growth of topological quantum materials is heavily dependent on reliable and proper synthesis methods. Indeed, the preparation of materials with distinct morphological features is usually studied, including bulk, film, and layered structures. To date, various synthesis techniques have been developed in experimental procedures: chemical vapor deposition (CVD), chemical vapor transport (CVT), and molecular beam epitaxy (MBE). In this chapter, the typical preparation methods of topological superconducting and topological magnetic materials are summarized.

### 2.1 Synthesis of bulk materials

In recent decades, the search for new topological superconducting and magnetic single crystal materials has been a challenging endeavor. Chemical vapor transport and the self-flux method are the two most common techniques for the synthesis of bulk single crystals.

#### 2.1.1 Chemical vapor transport

Top-down and bottom-up growth strategies are frequently employed to prepare two-dimensional materials<sup>[12]</sup>. Similar to CVD, the CVT technique is one of the most common

methods in the preparation of topological magnetic and topological superconducting materials. The CVT technique utilizes chemically reversible reactions to grow single crystals in different directions at different temperatures, which can be successfully applied for the syntheses of quantum materials<sup>[12–16]</sup>. A diagram of CVT synthesis and some single crystals grown using this procedure are depicted in Fig. 1.

It deserves special attention that the type of reaction is judged first to determine the crystal growth direction. Typically, in endothermic reactions, the raw materials are decomposed in the high-temperature region and deposited in the low-temperature region to form a single crystal, while the growth direction is the opposite in exothermic reactions<sup>[13]</sup>. In typical CVT synthesis, the raw materials and the selected transportation agent are sealed in an ampoule and placed in a high-temperature region. The transportation agent is then volatilized by heating, and a chemical reaction occurs between the raw materials and the transportation agent. When the reverse reaction occurs in the low-temperature region, a single crystal can be grown. During this process, the temperature is always controlled to achieve the purpose of controlling single crystal growth. The reactants are typically composed of raw materials and a selected transportation agent, such as iodine, chlorine, or hydrogen. A small amount of the transportation agent is often needed, as it does not enter into the growing crystal. In addition, an empirical dose of 3–5 mg/cm<sup>3</sup> is usually used.

The topological superconductor PbTaSe<sub>2</sub><sup>[17, 18]</sup>, for instance,

was grown by this method with PbCl<sub>2</sub> as a transport agent. Interestingly, PbTaSe<sub>2</sub> was found to be an intrinsic superconducting material with topological Dirac surface states, and its superconducting transition at a temperature of 3.8 K<sup>[17]</sup>. Superconducting bulk material SnTaSe<sub>2</sub> with  $T_c$  up to 3 K has drumhead-like surface states, offering an opportunity to explore the potential properties of such nodal-line semimetals<sup>[19]</sup>. In addition, single crystals of SmSbTe were grown by a two-step CVT method, which exhibits novel quantum properties originating from the interaction between topology, magnetism, and electronic correlations<sup>[20]</sup>. Meanwhile, MnBi<sub>2</sub>Te<sub>4</sub><sup>[21]</sup>, Fe<sub>3</sub>Sn<sub>2</sub><sup>[22, 23]</sup>, MnSb<sub>2</sub>Te<sub>4</sub><sup>[24, 25]</sup>, FeSe<sub>0.5</sub>Te<sub>0.5</sub><sup>[26–28]</sup>, Sn<sub>0.5</sub>TaSe<sub>2</sub><sup>[29]</sup>, Sr<sub>x</sub>Bi<sub>2</sub>Se<sub>3</sub><sup>[30–33]</sup>, Cu<sub>x</sub>Bi<sub>2</sub>Se<sub>3</sub><sup>[34–37]</sup>, Tl<sub>x</sub>Bi<sub>2</sub>Te<sub>3</sub><sup>[38, 39]</sup>, Nb<sub>x</sub>Bi<sub>2</sub>Se<sub>2</sub><sup>[40]</sup>, Co<sub>3</sub>Sn<sub>2</sub>S<sub>2</sub><sup>[41–43]</sup>, and Sn<sub>1-x</sub>In<sub>x</sub>Te<sup>[44]</sup>, as predicted to be possible topological superconducting or topological magnetic materials, could be realized by this synthesis method, providing a promising platform for the development of quantum information applications.

In summary, the CVT method provides an efficient method for the synthesis and further application of novel topological quantum materials and has become a powerful tool for exploring new topological superconducting and topological magnetic materials.

### 2.1.2 Self-flux method

The flux process is another effective means to synthesize single crystals from melt with the aid of flux<sup>[45]</sup>. The growth process involves dissolving the original composition of the

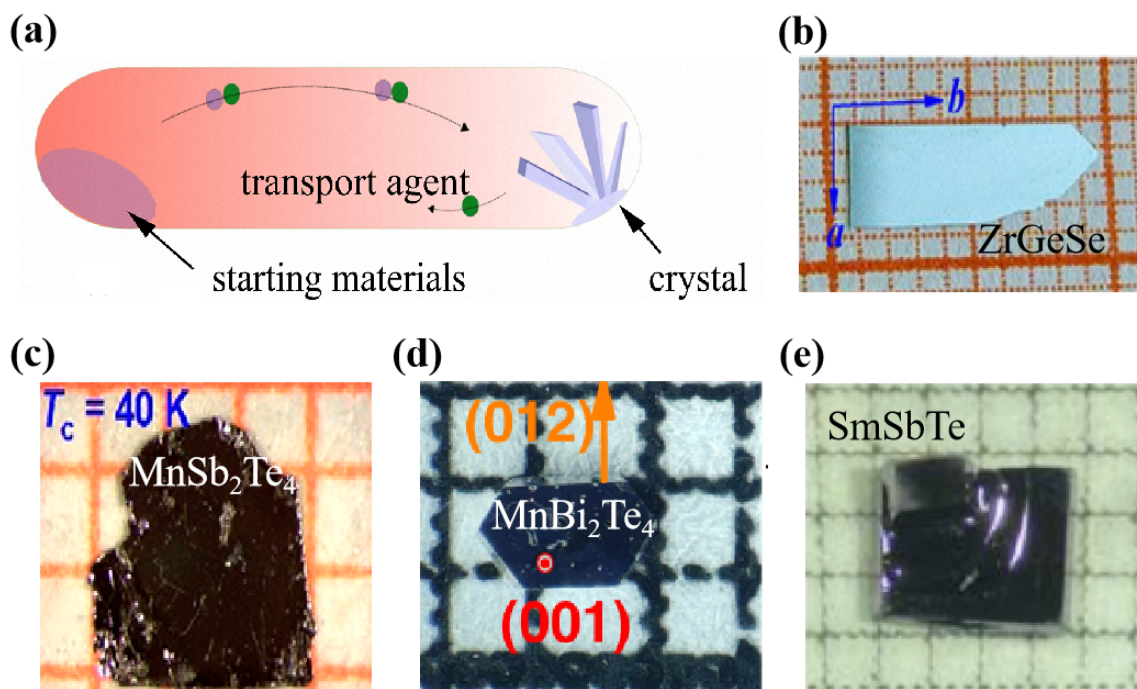


**Fig. 1.** (a) Schematic diagram for synthesizing single crystals by CVT technology and optical images of topological quantum single crystals grown by CVT. Reprinted with permission from Ref. [46]. Copyright 2017, American Physical Society. (b) ZrGeSe. Reprinted with permission from Ref. [47]. Copyright 2019, American Chemical Society. (c) MnSb<sub>2</sub>Te<sub>4</sub>. Reprinted with permission from Ref. [24]. Copyright 2022, American Chemical Society. (d) MnBi<sub>2</sub>Te<sub>4</sub>. Reprinted with permission from Ref. [21]. Copyright 2021, American Physical Society. (e) SmSbTe. Reprinted with permission from Ref. [20]. Copyright 2021, John Wiley & Sons, Inc.

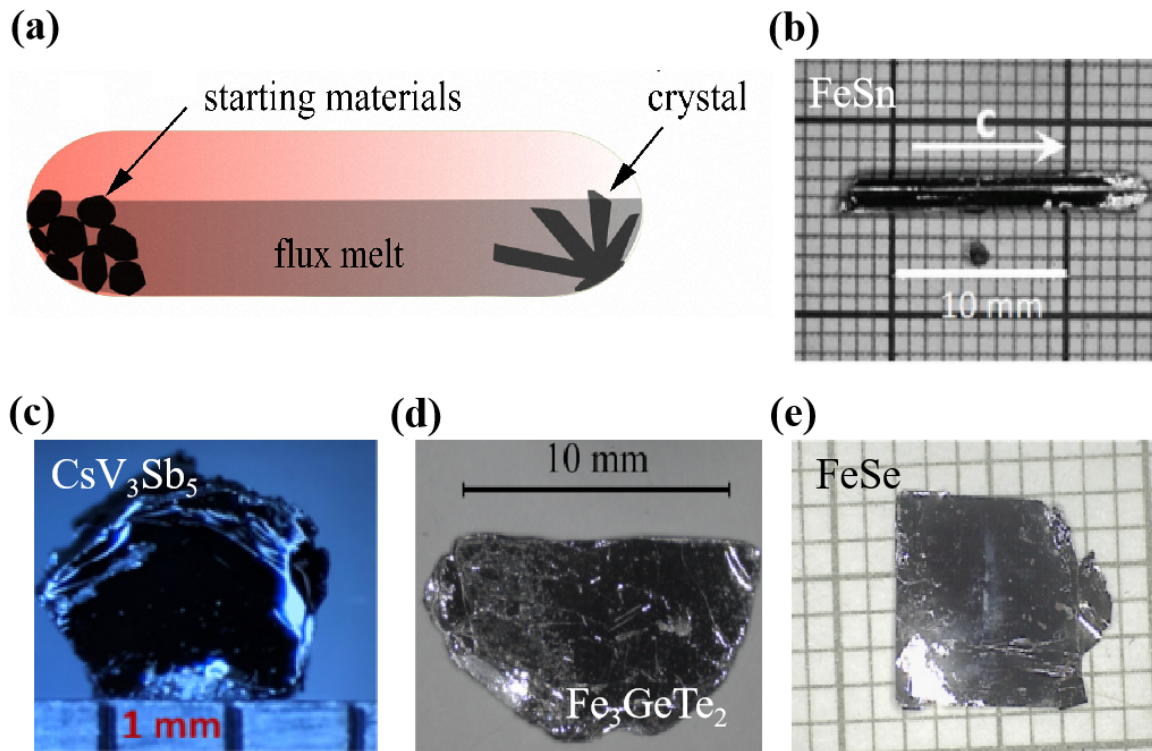


**Fig. 2.** (a) Illustration of the preparation of single crystals by the self-flux method and optical images of topological quantum materials. Reprinted with permission from Ref. [46]. Copyright 2017, American Physical Society. (b) FeSn. Reprinted with permission from Ref. [48]. Copyright 2019, American Physical Society. (c) CsV<sub>3</sub>Sb<sub>5</sub>. Reprinted with permission from Ref. [49]. Copyright 2022, American Physical Society. (d) Fe<sub>3</sub>GeTe<sub>2</sub>. Reprinted with permission from Ref. [50]. Copyright 2016, American Physical Society. (e) FeSe. Reprinted with permission from Ref. [46]. Copyright 2017, American Physical Society.

crystal in a low melting point flux solution at high temperature, forming a homogeneous saturated solution. Single crystals are then precipitated in a supersaturated solution by slow cooling. In the above procedures, the flux plays the leading role in the formation of single crystals, and self-flux is defined as the composition of the target compound, analogous to the conventional vertical flux growth process. Fig. 2 shows a diagram of this technique<sup>[46]</sup>.

Topological magnets and superconductors such as FeSn<sup>[48]</sup>, CoSn<sup>[51–53]</sup>, RhPb<sup>[53]</sup>, CsV<sub>3</sub>Sb<sub>5</sub><sup>[54–59]</sup>, KV<sub>3</sub>Sb<sub>5</sub><sup>[60–62]</sup>, Au<sub>2</sub>Pb<sup>[63, 64]</sup>, and TaIrTe<sub>4</sub><sup>[65]</sup> have been synthesized by this method. For the growth of the FeSn single crystal, the atomic ratio of Fe and Sn was 1 : 19, where the additional Sn element was used as a flux<sup>[48]</sup>. Single crystal CoSn was also prepared with an atomic ratio of Co : Sn of 1 : 9, whose flux was also the Sn element<sup>[51]</sup>. RhPb was grown from a lead flux with a molar ratio of 1 : 2, and the additional Pb-rich liquid was smoothly separated from the crystals by rapid spinning<sup>[53]</sup>. Moreover, the topological kagome superconductor CsV<sub>3</sub>Sb<sub>5</sub> was prepared by mixing Cs, V, and Sb in a molar ratio of 7 : 3 : 14 with a Cs–Sb binary eutectic mixture as the flux<sup>[59]</sup>. In summary, the self-flux method has been widely used for the preparation of topological kagome materials.

## 2.2 Synthesis of film materials

With the development of film deposition technology, the study of topological material systems has been accelerated.

However, the biggest challenge in low-dimensional quantum physics is how to grow high-quality topological quantum material thin films, which involves a series of issues related to thermodynamics, statistical mechanics, and condensed matter physics. A summary of some typical preparation procedures of film materials is presented below.

### 2.2.1 Chemical vapor deposition

Chemical vapor deposition (CVD), a conventional thin film technology, has also made great progress in the preparation of topological quantum materials<sup>[15]</sup>. In this method, one or more gaseous elements or compounds are usually used, and chemical reactions will be made on the surface of substrates to produce thin films. Specifically, the first step in this process is to place reactants and selected substrates into the two sides of the furnace. The reactants are then heated to form volatile substances, which drive the movement of reactants to the deposition areas. When chemical reactions and deposition occur on the surface of substrates, film samples are eventually obtained.

The procedure of the CVD method is well established, including normal pressure CVD<sup>[66]</sup>, photochemical CVD<sup>[67]</sup>, space restricted CVD<sup>[68]</sup>, plasma enhanced CVD<sup>[69–71]</sup>, CVD growth of salt-assisted or laser-assisted<sup>[72, 73]</sup>, pretreated precursor CVD growth, and so forth<sup>[74, 75]</sup>. Ordinary CVD procedures for preparing topological quantum materials are discussed in this section. He et al.<sup>[76]</sup> achieved controlled prepara-



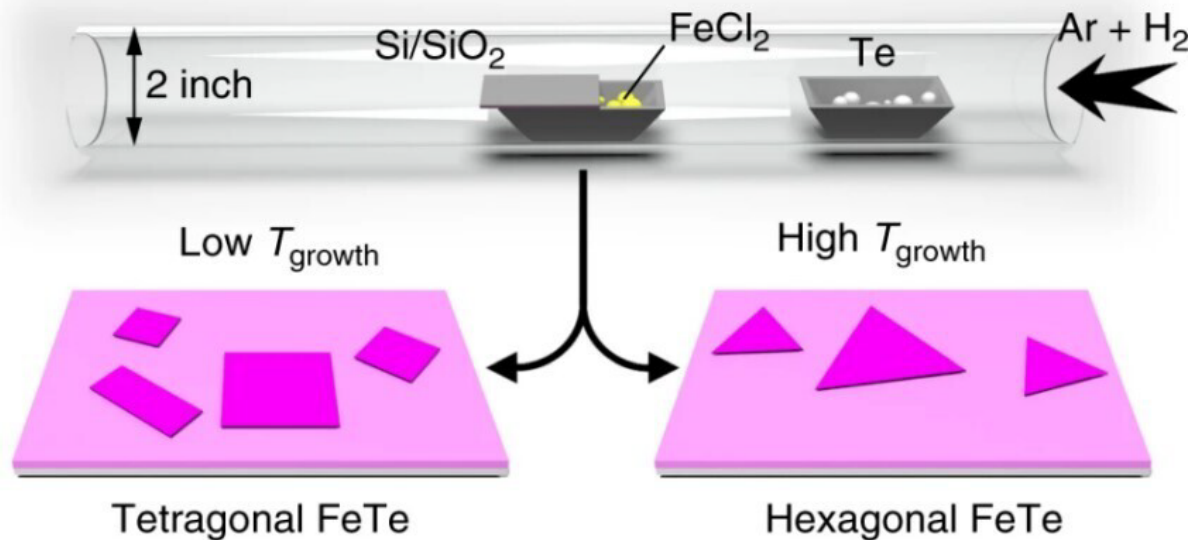


**Fig. 3.** Schematic diagram of FeTe material synthesis by the CVD method. Reprinted with permission from Ref. [77]. Copyright 2020. Springer Nature.

tion of CrSe, which is a candidate topological magnetic material, by using the normal pressure CVD method, and the results showed that CrSe exhibited significant ferromagnetism in both the in-plane and out-of-plane directions below 280 K. Liu's group<sup>[77]</sup> prepared FeTe on SiO<sub>2</sub>/Si substrates by using an ambient pressure CVD technique, as depicted in Fig. 3. During this growth procedure, FeCl<sub>2</sub> and Te powders were used as reactants, and mixtures of Ar and H<sub>2</sub> gas were introduced into the system from the right side of the tube. Under a fixed heating temperature of the tellurium source, tellurium vapor reacted with FeCl<sub>2</sub> at different growth temperatures to produce tetragonal and hexagonal FeTe. Moreover, the monolayer of FeTe was recently investigated to have the Dirac-cone-like topological electronic properties of nematic-like antiferromagnetic states by first-principles calculations<sup>[78]</sup>. Moreover, magnetic materials such as CoS<sub>2</sub><sup>[79–81]</sup>, CoSe<sub>2</sub><sup>[80, 81]</sup>, and MoS<sub>2</sub><sup>[82]</sup> have been successfully prepared and predicted to be possible topological materials.

### 2.2.2 Molecular beam epitaxy

Molecular beam epitaxy is a recent technology for the preparation of single-crystal films, which is appropriate for the study of low-dimensional quantum physics. Compared with CVD, MBE is capable of preparing single-crystal films with dozens of atomic layers, as well as ultrathin quantum functional films formed by alternating with different components and doping. The MBE method has been the first-rate technique for synthesizing ultrathin and defect-free quantum material films.

In a typical MBE technique, raw materials are heated in an ultrahigh vacuum furnace, forming a molecular beam that is ejected from the furnace and deposited on the single crystal substrate. The molecular beam is then controlled to scan the substrate, allowing molecules and atoms to grow on the substrate layer by layer according to the crystal arrangement to form a film. In 2017, Xiu's group<sup>[83]</sup> used the MBE technique to prepare large-size quantum material Fe<sub>3</sub>GeTe<sub>2</sub> thin films that were grown on (0001) sapphire and (111) GaAs and fur-

ther controlled the Curie temperature and coercivity by changing the concentration of Fe ions in Fe<sub>3</sub>GeTe<sub>2</sub>. They concluded that it opened an unprecedented platform to investigate possible physics when coupled with other superconductors and topological matter. In 2019, He et al.<sup>[84]</sup> used MBE to prepare topological magnetic material MnBi<sub>2</sub>Te<sub>4</sub> single-crystal thin films with intrinsic properties by alternately growing Bi<sub>2</sub>Te<sub>3</sub> and MnTe and excitedly observed the quantum anomalous Hall effect (QAHE). The ordered arrangement of magnetic atoms, large magnetic energy gap, and abundant topological phases make it an ideal system for searching the interaction between topology, magnetism, and other prospects. In 2021, topological superconductor Sr<sub>3</sub>SnO thin films were grown on a LaAlO<sub>3</sub> (001) substrate in Stemmer's group<sup>[85]</sup>, and they used the coevaporation of Sr and SnO<sub>2</sub> to form films with the MBE procedure. Additionally, Wang et al.<sup>[86]</sup> successfully synthesized Sn<sub>1-x</sub>In<sub>x</sub>Te thin films on a BaF<sub>2</sub> (111) substrate using the MBE method. They found that Sn<sub>1-x</sub>In<sub>x</sub>Te films exhibited superconducting fluctuations coexisting with quantum interference effects in conductivity above  $T_c$ . Furthermore, kagome magnet Fe<sub>3</sub>Sn<sub>2</sub> films were recently grown on a treated SrTiO<sub>3</sub> (111) substrate by the MBE technique<sup>[87]</sup>, which can offer a novel approach to growing kagome materials. In total, MBE technology has been widely used to prepare heterostructures, superlattices, and quantum wells, enabling the creation of topological materials with unique electronic and magnetic properties.

## 2.3 Synthesis of layered materials

### 2.3.1 Mechanical exfoliation

Mechanical exfoliation is the classic top-down method to obtain two-dimensional layered materials and is especially useful to exfoliate materials that have strong bonds within layers but weak van der Waals forces between layers. Since this method has a number of advantages, such as fewer defects, flat surface, and high mobility, it has been used to prepare topological quantum materials. To date, large numbers of mechanical exfoliation procedures have been applied in the exfoli-

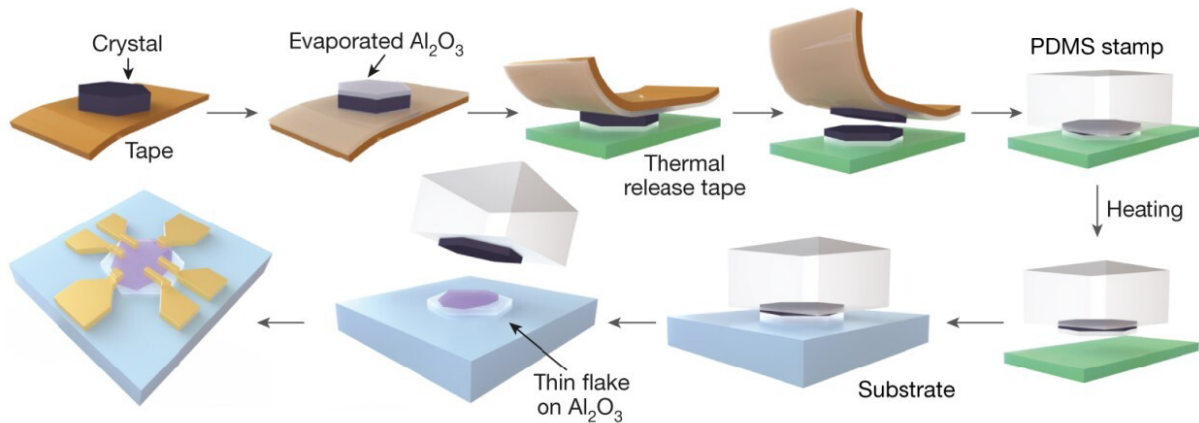


**Fig. 4.** Schematic diagram of  $\text{Al}_2\text{O}_3$ -assisted mechanical exfoliation of  $\text{Fe}_3\text{GeTe}_2$ . Reprinted with permission from Ref. [88]. Copyright 2018. Springer Nature.

ation of layered materials, including direct tape stripping,  $\text{Al}_2\text{O}_3$ -assisted exfoliation, plasma-assisted exfoliation, and gold-based exfoliation.

One of the most typical examples is the exfoliation of the quantum material  $\text{Fe}_3\text{GeTe}_2$ , and the process is shown in Fig. 4. Zhang et al.<sup>[88]</sup> developed an  $\text{Al}_2\text{O}_3$ -based auxiliary exfoliation method that used aluminum oxide as the skeleton to prevent the material from fragmenting during the exfoliation procedure to obtain a large area of single-layer samples. The specific process is to first steam a layer of aluminum oxide film on the surface of  $\text{Fe}_3\text{GeTe}_2$  and then stick the aluminum oxide layer and part of  $\text{Fe}_3\text{GeTe}_2$  together with the tape. After that, the sample was transferred to a PDMS thin film and pressed together to the silicon substrate. In the end,

$\text{Fe}_3\text{GeTe}_2$  samples with fewer layers or even monolayers were obtained. Additionally, other quantum materials, such as  $\text{CrGeTe}_3$ <sup>[89, 90]</sup>,  $\text{CrSiTe}_3$ <sup>[90]</sup>,  $\text{FePS}_3$ <sup>[91–93]</sup>,  $\text{MnPS}_3$ <sup>[94]</sup>, and  $\text{NiPS}_3$ <sup>[95, 96]</sup> are also exfoliated successfully.

However, this time-consuming approach cannot adjust the thickness of materials for deeper exploration and does not allow large-scale and high-yield output for electronic device applications.

### 2.3.2 Liquid phase exfoliation

Liquid phase exfoliation (LPE) is an available method for fabricating two-dimensional layered materials<sup>[15, 97]</sup>. This method involves the use of liquid solvents to separate the layers of materials, allowing for the desired creation of structures. A

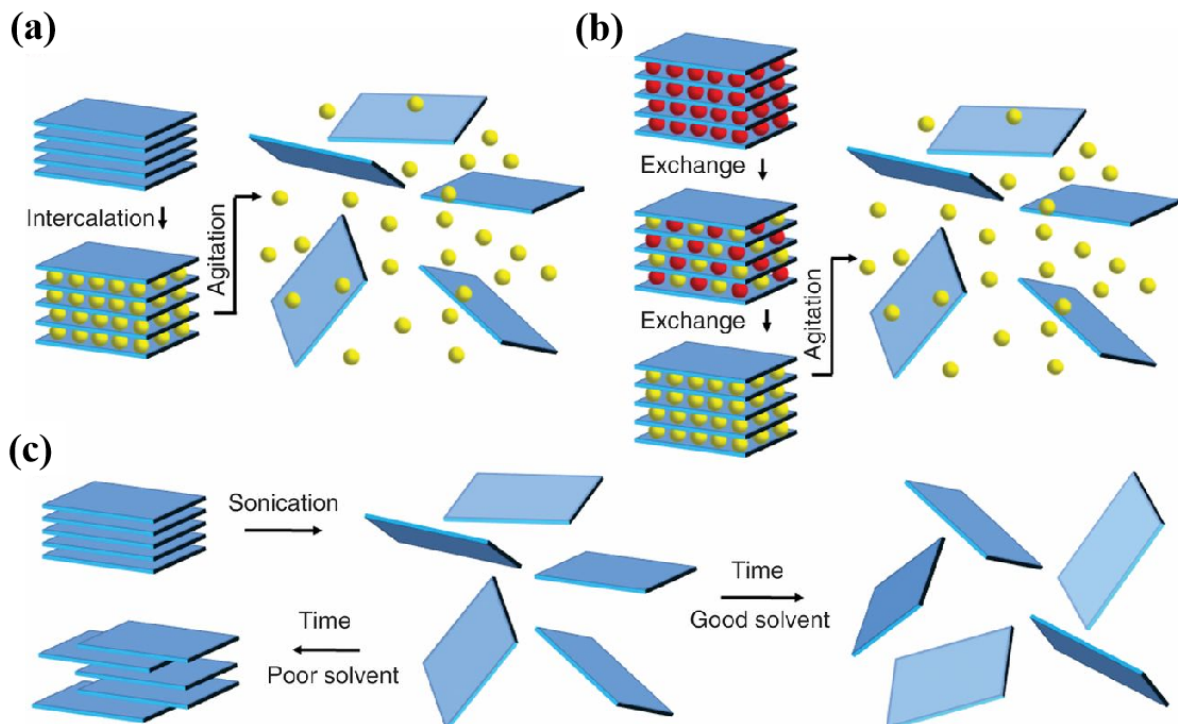


**Fig. 5.** Schematic illustration of different liquid exfoliation procedures: (a) intercalation, (b) ion exchange, and (c) ultrasonic exfoliation. Reprinted with permission from Ref. [98]. Copyright 2011. AAAS.

schematic presentation of the various liquid exfoliation procedures is depicted in Fig. 5<sup>[98]</sup>.

To date, the widely used means include ultrasonication, intercalation, and ion exchange methods. Due to the peak yield and mild conditions, LPE may be used as a feasible preparation of topological quantum materials. Different thick FeSe films were grown on insulating substrates such as strontium titanate and magnesium oxide by using a pulsed-laser deposition technique, and the films were covered with the ionic liquid. Then, this group applied the electrochemical etching method to exfoliate FeSe layers to investigate the superconductivity in FeSe<sup>[99]</sup>. In addition, topological superconductor TaSe<sub>2</sub> layers were obtained from TaSe<sub>2</sub> bulk using the LPE method, where the bulk material was mixed with N-methyl-2-pyrrolidone and subjected to ultrasonic treatment to obtain TaSe<sub>2</sub> layers<sup>[100]</sup>. Recently, Zhan's group prepared few-layer ZrTe<sub>3</sub> nanosheets using the LPE technique by grinding bulk ZrTe<sub>3</sub> and mixing it with an alcohol solution, followed by ultrasonic exfoliation<sup>[101]</sup>. While LPE has been used to prepare layers and nanosheets, it is still less common in the preparation of topological materials.

#### 2.4 Synthesis of materials with other morphological features

Additionally, there are some growth methods, such as CVT, CVD, and LPE, that can prepare other morphologies of materials, for instance, wires, rods, ribbons, and flakes. These methods are indispensable for probing topological quantum materials. Furthermore, these methods can also be used to create nanostructures that are materials with dimensions on the nanoscale, which are the tool to study the effects of size and shape on the topological properties of the materials. Now some of them are discussed as below.

Topological materials Bi<sub>2</sub>Te<sub>3</sub>, In<sub>2</sub>Se<sub>3</sub>, Sb<sub>2</sub>Te<sub>3</sub>, and GaSe nanowires and nanoribbons have been synthesized by the vapor-liquid-solid (VLS) technique, which is a combined growth method involving the existence of three states of gas, liquid, and solid. First, the target materials change from the gas state to the liquid state and then deposit on the substrate to grow crystals. Kong et al. discussed high-quality Bi<sub>2</sub>Se<sub>3</sub> nanowires and nanoribbons employing the Au-catalyzed VLS method and found that Bi<sub>2</sub>Se<sub>3</sub> nanowires were composed of axial stacking along the wires and that Bi<sub>2</sub>Se<sub>3</sub> nanoribbons even had various dimensional morphologies<sup>[102]</sup>.

### 3 Properties and applications of topological quantum materials

Topology is a mathematical concept that refers to insensitivity to detail and continuous change. For example, if a donut has a hole in it, then the number of holes is a topological feature that distinguishes two dimensions in a three-dimensional space, which is the classical interpretation of topology. In addition, topology can also be used to describe the properties of materials, such as the arrangement of atoms in a crystal lattice or the electronic structure of materials. This type of topology is known as topological quantum materials, which exhibit unique properties due to their topological structure.

#### 3.1 Properties and applications of topological magnets

The discovery of the integer quantum Hall effect (IQHE) and fractional quantum Hall effect (FQHE) has revealed a novel kind of matter: the topological quantum state. To study the topological properties of these materials is to find similar topological characteristics in the electronic band structures and the physical quantities or quantum states determined by these characteristics to obtain the physical properties or quantum states that are not sensitive to the details of the defects and impurity energy of the materials. To explore these properties and quantum states, angle-resolved photoemission spectroscopy (ARPES) plays a key role in discovering and understanding topological phases by identifying nontrivial topological electronic structures<sup>[103]</sup>. Additionally, ARPES can also be used to measure the topological invariants of the materials, which are the numerical values that characterize the topological properties of quantum materials. These topological invariants are often used to classify different topological phases and to study the effects of external perturbations on the topological properties of materials.

A classic example is the topological magnet CoSn<sub>2</sub>S<sub>2</sub> with a fascinating kagome lattice structure<sup>[42]</sup>. The optical image of topological magnet Co<sub>3</sub>Sn<sub>2</sub>S<sub>2</sub> is shown in Fig. 6a<sup>[104]</sup>. Studies have shown that this typical Weyl semimetal with broken time reversal symmetry (TRS) exhibits a high ferromagnetic transition at temperatures of 175–177 K. Fig. 6b illustrates the typical magnetic properties of Co<sub>3</sub>Sn<sub>2</sub>S<sub>2</sub> single crystals. The  $\chi(T)$  curves in the ZFC and FC modes at  $\mu_0H = 1$  T with  $H||c$  exhibit a sharp increase below the Curie temperature. The  $M(\mu_0H)$  curve demonstrates a significant hysteresis with a square-shaped loop that reverses direction at a minimal coercive field  $\mu_0H_c$ <sup>[105]</sup>. Fig. 6c and d depict the Brillouin zones of the Co<sub>3</sub>Sn<sub>2</sub>S<sub>2</sub> samples and their ARPES spectra, respectively. The distinct triangular states around the  $K$  point and several broad regions of spectral weight, particularly around the  $M$  point, are revealed, where a possible topological Fermi arc is represented with a white arrow<sup>[106]</sup>. These potential physical properties can bring some fascinating applications in storage; for example, sodium ion capacitors based on the Co<sub>3</sub>Sn<sub>2</sub>S<sub>2</sub>-carbon nanoi-ion anode maintain a superior capacity retention and enhanced cycle life compared with other anode materials<sup>[107]</sup>. This provides a new perspective on utilizing topological magnets as anodes for high-rate sodium ion storage.

The observation of the quantum anomalous Hall effect (QAHE) has always been a significant aspect in the discovery of topological magnetic materials because the dissipative edge states in the QHE are especially beneficial for the applications of low-energy electronics and the implementation of topological superconducting quantum computation. In fact, scientists are now still trying to raise the critical temperature of the QAHE, and several topological materials predicted by high-throughput calculations have made them potential materials for studying QAHE phases. This could pave the way for the creation of high-temperature QAHE materials and create favorable conditions for further research on topological magnets. Furthermore, the rich magnetic properties in topological magnetic materials have incredible properties; for instance, chiral channels that support electrons and spins have vast



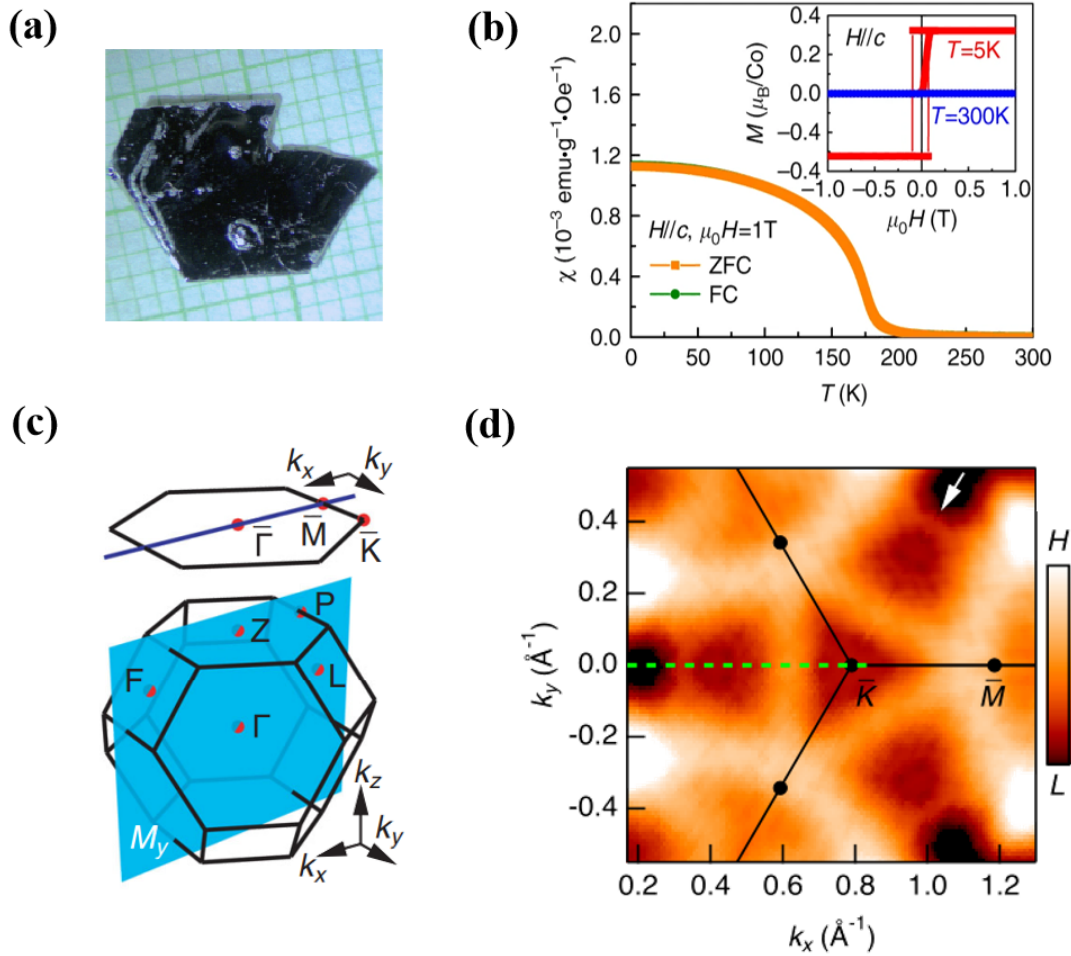


**Fig. 6.** (a) Photo of  $\text{Co}_3\text{Sn}_2\text{S}_2$  single crystals. Reprinted with permission from Ref. [104]. Copyright 2023, IOP Publishing. (b) Temperature dependence of magnetic susceptibility with ZFC and FC modes at  $\mu_0 H = 1$  T with  $H||c$ . Inset: field dependence of magnetization at 5 and 300 K for  $H||c$ . Reprinted with permission from Ref. [105]. Copyright 2018, Springer Nature. (c) The Brillouin zones of  $\text{Co}_3\text{Sn}_2\text{S}_2$  for the bulk and (111) surface with several high-symmetry points marked in red. Reprinted with permission from Ref. [106]. Copyright 2021, American Physical Society. (d) The Fermi surface in the vicinity of the  $\bar{K}$  point by using ARPES, where white arrows indicate a potential topological Fermi arc. Reprinted with permission from Ref. [106]. Copyright 2021, American Physical Society.

potential for development applications, including information storage, control of dissipation-free spin, charge transport and the response to external stimuli such as light and temperature. These properties have enabled the development of various spintronics devices, including spin valves, spin orbit torque, and spin field effect transistors.

### 3.2 Properties and applications of topological superconductors

The observation of topological states has been described previously for topological superconducting materials, so a physical property measurement system (PPMS) is an excellent tool to determine the presence of superconductivity in topological superconducting candidates<sup>[10]</sup>. The transition has always occurred in the temperature-dependent resistance, magnetization, and heat capacity of superconducting materials, and the temperature-dependent heat capacity measurement is considered to be a reliable way to determine the properties of superconductors. Additionally, there are many other methods

for the characterization of topological superconducting materials that are not listed in detail due to limited space.

Here, the superconductor  $\text{PbTaSe}_2$  with topological surface states is taken as an example<sup>[17]</sup>. As illustrated in Fig. 7, there exist bulk band pockets surrounding  $\Gamma$  and  $K$  at the Fermi level, but the topological surface states encircling  $\Gamma$  are not degenerate with these bulk bands, showing an isolated surface band with helical spin texture. Due to this hybridization with bulk states and spin-momentum locking of the surface states, helical topological superconductivity can be induced on the surface.

The combination of topology and superconductivity will form a new quantum state, a topological superconductor, and this material has become one of the most concerning topics in quantum computing. To date, the main challenge in implementing large-scale quantum computing is the need to avoid errors due to decoherence effects caused by perturbation. Compared with traditional quantum computing schemes, topological quantum computing may fundamentally solve this



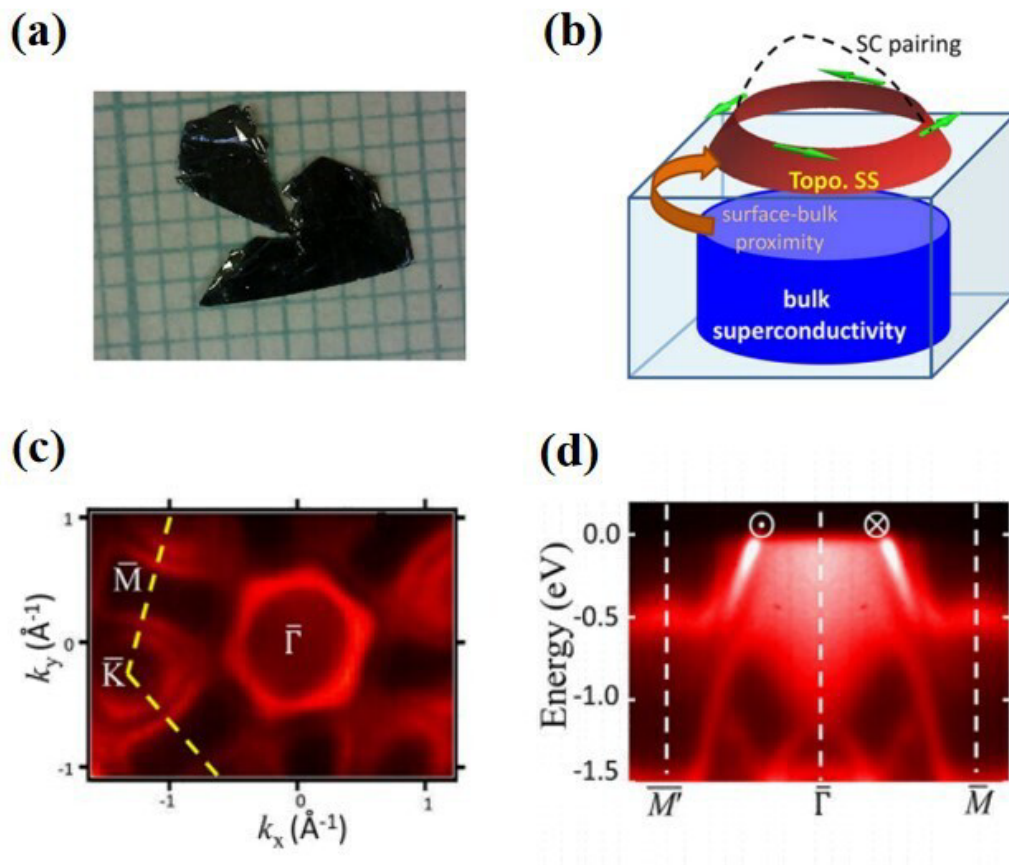


**Fig. 7.** (a) Optical image of PbTaSe<sub>2</sub> single crystals. (b) The diagram of helical Cooper pairing as the result of the surface-bulk proximity effect. (c) ARPES Fermi surface taken with 64 eV photons. (d) ARPES spectral cut along  $\bar{M}'$ - $\bar{\Gamma}$ - $\bar{M}$ . Reprinted with permission from Ref. [17]. Copyright 2016. American Physical Society.

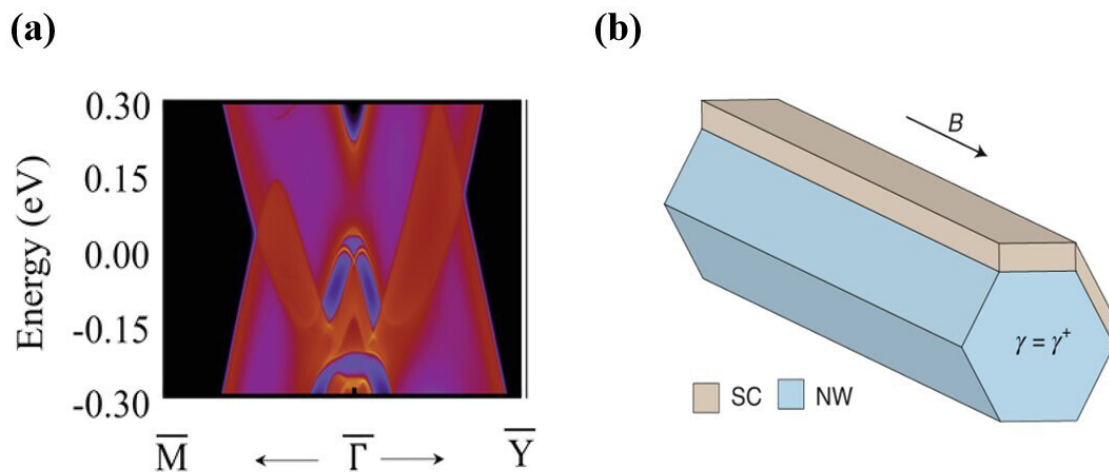


**Fig. 8.** (a) Topological surface states of 2 M-WS<sub>2</sub>, reprinted with permission from Ref. [108], copyright 2019, John Wiley & Sons, Inc. (b) Schematic diagram of the spin-orbit semiconductor nanowire coupled to the S-wave superconductor in an external magnetic field  $B$ . Majorana zero modes  $\gamma$  are expected at the ends of the heterogeneous nanowire, reprinted with permission from Ref. [109], copyright 2020, Springer Nature.

problem, making topological superconductors the basis of topological quantum computing. In addition, it has long been predicted that the surface may exhibit a Majorana zero-

energy mode in topological superconducting materials, which provides the possibility for topological quantum computation with high fault tolerance. Currently, the topological

properties of other quantum materials have been successfully observed. For instance, as shown in Fig. 8a, anisotropic Majorana bound states were recently observed in magnetic vortices within the topological superconductor 2 M-WS<sub>2</sub><sup>[108]</sup>, which may originate from the anisotropy of the superconducting order parameter and topological surface states. The discovery of this topological property has the potential to enable the construction of novel heterostructures and establish a robust platform for further investigation into Majorana bound states. At present, topological superconductivity has been detected in several material systems, with semiconductor-superconductor heterogeneous nanowires being the most promising candidate. Studies have described that the emergence of Majorana fermions in these nanowires may result from the coupling of S-wave superconductors with strongly spin-orbit-coupled semiconductor nanowires<sup>[109]</sup>, as illustrated in Fig. 8b. The compatibility of nanowires with available technologies in material preparation and device processing, along with their feasibility for achieving non-Abelian braiding and topological quantum computing, has made them a subject of mainstream research worldwide. However, to advance other topological superconductor candidates for quantum computing and develop stable qubit modules, further understanding of the physical properties of Majorana fermions will still be needed.

## 4 Summary and outlook

Topological quantum materials have the potential to revolutionize condensed matter physics and electronic device applications. To fully realize the exotic quantum phenomenon of these materials, it is essential to obtain high-quality materials that are based on energy band theory. In this paper, the synthesis, properties, and applications of topological quantum materials are reviewed, and we also find that many challenges still need to be addressed. For instance, a large quantity of predicted topological materials have yet to be experimentally verified, such as Sc<sub>2</sub>CrB<sub>6</sub><sup>[110]</sup>, SbV<sub>3</sub>S<sub>5</sub><sup>[111]</sup>, and NbRu<sub>3</sub>C<sup>[112]</sup>. Furthermore, the number of high-quality and stable quantum material systems is still limited. To further advance the development of topological quantum materials, it is necessary to explore materials that are stable in air and have better performance. In summary, topological quantum materials may facilitate the industrial development of electronics, spintronics, and other subjects in the foreseeable future.

## Acknowledgements

This work was supported by National Natural Science Foundation of China (52373309).

## Conflict of interest

The authors declare that they have no conflict of interest.

## Biographies

**Junjie Wu** is currently a postgraduate student at the University of Science and Technology of China. His research focuses on the synthesis and properties of topological quantum materials.

**Bin Xiang** is a Professor at the University of Science and Technology of China. He received his Ph.D. degree from Peking University in 2005. His research field includes the synthesis, characterization and application of two-dimensional quantum functional materials.

## References

- [1] Klitzing K V, Dorda G, Pepper M. New method for high-accuracy determination of the fine-structure constant based on quantized Hall resistance. *Physical Review Letters*, **1980**, *45*: 494–497.
- [2] Lv B Q, Qian T, Ding H. Experimental perspective on three-dimensional topological semimetals. *Reviews of Modern Physics*, **2021**, *93*: 025002.
- [3] Sato M, Ando Y. Topological superconductors: A review. *Reports on Progress in Physics*, **2017**, *80*: 076501.
- [4] Read N, Green D. Paired states of fermions in two dimensions with breaking of parity and time-reversal symmetries and the fractional quantum Hall effect. *Physical Review B*, **2000**, *61*: 10267–10297.
- [5] Kitaev A Y. Unpaired Majorana fermions in quantum wires. *Physics-Uspeski*, **2001**, *44*: 131.
- [6] Nayak C, Simon S H, Stern A, et al. Non-Abelian anyons and topological quantum computation. *Reviews of Modern Physics*, **2008**, *80*: 1083–1159.
- [7] Xu Y, Elcoro L, Song Z D, et al. High-throughput calculations of magnetic topological materials. *Nature*, **2020**, *586*: 702–707.
- [8] Morali N, Batabyal R, Nag P K, et al. Fermi-arc diversity on surface terminations of the magnetic Weyl semimetal Co<sub>3</sub>Sn<sub>2</sub>S<sub>2</sub>. *Science*, **2019**, *365*: 1286–1291.
- [9] Noky J, Zhang Y, Gooth J, et al. Giant anomalous Hall and Nernst effect in magnetic cubic Heusler compounds. *npj Computational Materials*, **2020**, *6*: 77.
- [10] Sharma M M, Sharma P, Karn N K, et al. Comprehensive review on topological superconducting materials and interfaces. *Superconductor Science and Technology*, **2022**, *35*: 083003.
- [11] Bernevig B A, Felser C, Beidenkopf H. Progress and prospects in magnetic topological materials. *Nature*, **2022**, *603*: 41–51.
- [12] Reale F, Sharda K, Mattevi C. From bulk crystals to atomically thin layers of group VI-transition metal dichalcogenides vapour phase synthesis. *Applied Materials Today*, **2016**, *3*: 11–22.
- [13] Wang D, Luo F, Lu M, et al. Chemical vapor transport reactions for synthesizing layered materials and their 2D counterparts. *Small*, **2019**, *15*: 1804404.
- [14] Das S, Kim M, Lee J W, et al. Synthesis, properties, and applications of 2-D materials: A comprehensive review. *Critical Reviews in Solid State and Materials Sciences*, **2014**, *39*: 231–252.
- [15] Özel F, Arkan E, Coskun H, et al. Refractory-metal-based chalcogenides for energy. *Advanced Functional Materials*, **2022**, *32*: 2207705.
- [16] Binnewies M, Glaum R, Schmidt M, et al. Chemical vapor transport reactions—A historical review. *Zeitschrift Für Anorganische Und Allgemeine Chemie*, **2013**, *639*: 219–229.
- [17] Chang T R, Chen P J, Bian G, et al. Topological Dirac surface states and superconducting pairing correlations in PbTaSe<sub>2</sub>. *Physical Review B*, **2016**, *93*: 245130.
- [18] Bian G, Chang T R, Sankar R, et al. Topological nodal-line fermions in spin-orbit metal PbTaSe<sub>2</sub>. *Nature Communications*, **2016**, *7* (1): 10556.
- [19] Chen W, Liu L, Yang W, et al. Evidence of topological nodal lines and surface states in the centrosymmetric superconductor SnTaS<sub>2</sub>. *Physical Review B*, **2021**, *103*: 035133.
- [20] Pandey K, Mondal D, Villanova J W, et al. Magnetic topological semimetal phase with electronic correlation enhancement in SmSbTe. *Advanced Quantum Technologies*, **2021**, *4* (10): 2100063.
- [21] Hu C, Gao A, Berggren B S, et al. Growth, characterization and Chern insulator state in MnBi<sub>2</sub>Te<sub>4</sub> via the chemical vapor transport method. *Physical Review Materials*, **2021**, *5* (12): 124206.
- [22] Zhang H, Xu C Q, Ke X. Topological Nernst effect, anomalous Nernst effect, and anomalous thermal Hall effect in the Dirac

- semimetal  $\text{Fe}_3\text{Sn}_2$ . *Physical Review B*, **2021**, *103*: L201101.
- [23] Berry T, Ng N, McQueen T M. Single crystal growth tricks and treats. arXiv: 2209.09370, **2022**.
- [24] Xi M, Chen F, Gong C, et al. Relationship between antisite defects, magnetism, and band topology in  $\text{MnSb}_2\text{Te}_4$  crystals with  $T_C \approx 40$  K. *The Journal of Physical Chemistry Letters*, **2022**, *13*: 10897–10904.
- [25] Murakami T, Nambu Y, Koretsune T, et al. Realization of interlayer ferromagnetic interaction in  $\text{MnSb}_2\text{Te}_4$  toward the magnetic Weyl semimetal state. *Physical Review B*, **2019**, *100*: 195103.
- [26] Liu S B, Yuan J, Huh S, et al. Electronic phase diagram of iron chalcogenide superconductors  $\text{FeSe}_{1-x}\text{S}_x$  and  $\text{FeSe}_{1-y}\text{Te}_y$ . arXiv: 2009.13286, **2020**.
- [27] Wang Z, Zhang P, Xu G, et al. Topological nature of the  $\text{FeSe}_{0.5}\text{Te}_{0.5}$  superconductor. *Physical Review B*, **2015**, *92*: 115119.
- [28] Yang Y, Feng S Q, Xiang Y Y, et al. Comparison of band structure and superconductivity in  $\text{FeSe}_{0.5}\text{Te}_{0.5}$  and  $\text{FeS}$ . *Chinese Physics B*, **2017**, *26*: 127401.
- [29] Adam M L, Liu Z, Moses O A, et al. Superconducting properties and topological nodal lines features in centrosymmetric  $\text{Sn}_{0.5}\text{TaSe}_2$ . *Nano Research*, **2021**, *14*: 2613–2619.
- [30] Li M, Fang Y, Pei C, et al. Phonon softening and higher-order anharmonic effect in the superconducting topological insulator  $\text{Sr}_x\text{Bi}_2\text{Se}_3$ . *Journal of Physics: Condensed Matter*, **2020**, *32*: 385701.
- [31] Liu Z, Yao X, Shao J, et al. Superconductivity with topological surface state in  $\text{Sr}_x\text{Bi}_2\text{Se}_3$ . *Journal of the American Chemical Society*, **2015**, *137* (33): 10512–10515.
- [32] Du G, Shao J, Yang X, et al. Drive the Dirac electrons into Cooper pairs in  $\text{Sr}_x\text{Bi}_2\text{Se}_3$ . *Nature Communications*, **2017**, *8* (1): 14466.
- [33] Han C Q, Li H, Chen W J, et al. Electronic structure of a superconducting topological insulator Sr-doped  $\text{Bi}_2\text{Se}_3$ . *Applied Physics Letters*, **2015**, *107*: 171602.
- [34] Hor Y S, Williams A J, Checkelsky J G, et al. Superconductivity in  $\text{Cu}_x\text{Bi}_2\text{Se}_3$  and its implications for pairing in the undoped topological insulator. *Physical Review Letters*, **2010**, *104*: 057001.
- [35] Kriener M, Segawa K, Ren Z, et al. Bulk superconducting phase with a full energy gap in the doped topological insulator  $\text{Cu}_x\text{Bi}_2\text{Se}_3$ . *Physical Review Letters*, **2011**, *106* (12): 127004.
- [36] Wray L A, Xu S-Y, Xia Y, et al. Observation of topological order in a superconducting doped topological insulator. *Nature Physics*, **2010**, *6* (11): 855–859.
- [37] Kriener M, Segawa K, Ren Z, et al. , Electrochemical synthesis and superconducting phase diagram of  $\text{Cu}_x\text{Bi}_2\text{Se}_3$ . *Physical Review B*, **2011**, *84* (5): 054513.
- [38] Trang C X, Wang Z, Takane D, et al. Fermiology of possible topological superconductor  $\text{Tl}_{0.5}\text{Bi}_2\text{Te}_3$  derived from hole-doped topological insulator. *Physical Review B*, **2016**, *93* (24): 241103.
- [39] Venderbos J W F, Kozii V, Fu L. Identification of nematic superconductivity from the upper critical field. *Physical Review B*, **2016**, *94*: 094522.
- [40] Qiu Y S, Sanders K N, Dai J X, et al. Time reversal symmetry breaking superconductivity in topological materials. arXiv: 1512.03519, **2015**.
- [41] Tanaka M, Fujishiro Y, Mogi M, et al. Topological kagome magnet  $\text{Co}_3\text{Sn}_2\text{S}_2$  thin flakes with high electron mobility and large anomalous Hall effect. *Nano Letters*, **2020**, *20* (10): 7476–7481.
- [42] Kanagaraj M, Ning J, He L. Topological  $\text{Co}_3\text{Sn}_2\text{S}_2$  magnetic Weyl semimetal: From fundamental understanding to diverse fields of study. *Reviews in Physics*, **2022**, *8*: 100072.
- [43] Ding L, Koo J, Xu L, et al. Intrinsic anomalous Nernst effect amplified by disorder in a half-metallic semimetal. *Physical Review X*, **2019**, *9* (4): 041061.
- [44] Sasaki S, Ren Z, Taskin A A, et al. Odd-parity pairing and topological superconductivity in a strongly spin-orbit coupled semiconductor. *Physical Review Letters*, **2012**, *109* (21): 217004.
- [45] Kanatzidis M G, Pöttgen R, Jeitschko W. The metal flux: A preparative tool for the exploration of intermetallic compounds. *Angewandte Chemie International Edition*, **2005**, *44*: 6996–7023.
- [46] Yan J Q, Sales B C, Susner M A, et al. Flux growth in a horizontal configuration: An analog to vapor transport growth. *Physical Review Materials*, **2017**, *1*: 023402.
- [47] Guo L, Chen T W, Chen C, et al. Electronic transport evidence for topological nodal-line semimetals of  $\text{ZrGeSe}$  single crystals. *ACS Applied Electronic Materials*, **2019**, *1*: 869–876.
- [48] Sales B C, Yan J, Meier W R, et al. Electronic, magnetic, and thermodynamic properties of the kagome layer compound  $\text{FeSn}$ . *Physical Review Materials*, **2019**, *3*: 114203.
- [49] Shrestha K, Chapai R, Pokharel B K, et al. Nontrivial Fermi surface topology of the kagome superconductor  $\text{CsV}_3\text{Sb}_5$  probed by de Haas-van Alphen oscillations. *Physical Review B*, **2022**, *105*: 024508.
- [50] May A F, Calder S, Cantoni C, et al. Magnetic structure and phase stability of the van der Waals bonded ferromagnet  $\text{Fe}_{3-x}\text{GeTe}_2$ . *Physical Review B*, **2016**, *93*: 014411.
- [51] Kang M, Fang S, Ye L, et al. Topological flat bands in frustrated kagome lattice  $\text{CoSn}$ . *Nature Communications*, **2020**, *11*: 4004.
- [52] Liu Z, Li M, Wang Q, et al. Orbital-selective Dirac fermions and extremely flat bands in frustrated kagome-lattice metal  $\text{CoSn}$ . *Nature Communications*, **2020**, *11*: 4002.
- [53] Meier W R, Du M H, Okamoto S, et al. Flat bands in the  $\text{CoSn}$ -type compounds. *Physical Review B*, **2020**, *102*: 075148.
- [54] Zhao H, Li H, Ortiz B R, et al. Cascade of correlated electron states in the kagome superconductor  $\text{CsV}_3\text{Sb}_5$ . *Nature*, **2021**, *599*: 216–221.
- [55] Zhao C C, Wang L X, Xia W, et al., Nodal superconductivity and superconducting dome in the topological Kagome metal  $\text{CsV}_3\text{Sb}_5$ . arXiv:2102.08356, **2021**.
- [56] Kang M, Fang S, Kim J K, et al. Twofold van Hove singularity and origin of charge order in topological kagome superconductor  $\text{CsV}_3\text{Sb}_5$ . *Nature Physics*, **2022**, *18*: 301–308.
- [57] Gupta R, Das D, Mielke III C H, et al. Microscopic evidence for anisotropic multigap superconductivity in the  $\text{CsV}_3\text{Sb}_5$  kagome superconductor. *npj Quantum Materials*, **2022**, *7*: 49.
- [58] Ge J, Wang P Y, Xing Y, et al. Discovery of charge-4e and charge-6e superconductivity in kagome superconductor  $\text{CsV}_3\text{Sb}_5$ . arXiv: 2201.10352, **2022**.
- [59] Xiang Y, Li Q, Li Y, et al. Twofold symmetry of c-axis resistivity in topological kagome superconductor  $\text{CsV}_3\text{Sb}_5$  with in-plane rotating magnetic field. *Nature Communications*, **2021**, *12* (1): 6727.
- [60] Jiang Y X, Yin J X, Denner M M, et al. Unconventional chiral charge order in kagome superconductor  $\text{KV}_3\text{Sb}_5$ . *Nature Materials*, **2021**, *20* (10): 1353–1357.
- [61] Li H, Zhao H, Ortiz B R, et al. Rotation symmetry breaking in the normal state of a kagome superconductor  $\text{KV}_3\text{Sb}_5$ . *Nature Physics*, **2022**, *18* (3): 265–270.
- [62] Jiang K, Wu T, Yin J X, et al. Kagome superconductors  $\text{AV}_3\text{Sb}_5$  (A = K, Rb, Cs). *National Science Review*, **2023**, *10* (2): nwac199.
- [63] Xing Y, Wang H, Li C K, et al. Superconductivity in topologically nontrivial material  $\text{Au}_2\text{Pb}$ . *npj Quantum Materials*, **2016**, *1*: 16005.
- [64] Schoop L M, Xie L S, Chen R, et al. Dirac metal to topological metal transition at a structural phase change in  $\text{Au}_2\text{Pb}$  and prediction of Z2 topology for the superconductor. *Physical Review B*, **2015**, *91*: 214517.
- [65] Xing Y, Shao Z, Ge J, et al. Surface superconductivity in the type II Weyl semimetal  $\text{TaIrTe}_4$ . *National Science Review*, **2020**, *7* (3): 579–587.
- [66] Yu J, Li J, Zhang W, et al. Synthesis of high quality two-dimensional materials via chemical vapor deposition. *Chemical Science*, **2015**, *6* (12): 6705–6716.
- [67] Saitoh T, Muramatsu S, Shimada T, et al. Optical and electrical properties of amorphous silicon films prepared by photochemical vapor deposition. *Applied Physics Letters*, **1983**, *42* (8): 678–679.
- [68] Zhou S, Wang R, Han J, et al. Ultrathin non-van der Waals



- magnetic rhombohedral  $\text{Cr}_2\text{S}_3$ : Space-confined chemical vapor deposition synthesis and Raman scattering investigation. *Advanced Functional Materials*, **2019**, 29 (3): 1805880.
- [69] Yi K, Liu D, Chen X, et al. Plasma-enhanced chemical vapor deposition of two-dimensional materials for applications. *Accounts of Chemical Research*, **2021**, 54 (4): 1011–1022.
- [70] Lucovsky G, Tsu D V. Plasma enhanced chemical vapor deposition: Differences between direct and remote plasma excitation. *Journal of Vacuum Science & Technology A: Vacuum, Surfaces, and Films*, **1987**, 5 (4): 2231–2238.
- [71] Hess D W. Plasma-enhanced CVD: Oxides, nitrides, transition metals, and transition metal silicides. *Journal of Vacuum Science & Technology A: Vacuum, Surfaces, and Films*, **1984**, 2 (2): 244–252.
- [72] Zhou J, Lin J, Huang X, et al. A library of atomically thin metal chalcogenides. *Nature*, **2018**, 556: 355–359.
- [73] Demiryont H, Thompson L R, Collins G J. Optical properties of aluminum oxynitrides deposited by laser-assisted CVD. *Applied Optics*, **1986**, 25: 1311.
- [74] Xu H, Wei J, Zhou H, et al. High spin Hall conductivity in large-area type-II Dirac semimetal  $\text{PtTe}_2$ . *Advanced Materials*, **2020**, 32 (17): e2000513.
- [75] Wang L, Xu C, Liu Z, et al. Magnetotransport properties in high-quality ultrathin two-dimensional superconducting  $\text{Mo}_2\text{C}$  crystals. *ACS Nano*, **2016**, 10 (4): 4504–4510.
- [76] Zhang Y, Chu J, Yin L, et al. Ultrathin magnetic 2D single-crystal  $\text{CrSe}$ . *Advanced Materials*, **2019**, 31 (19): 1900056.
- [77] Kang L, Ye C, Zhao X, et al. Phase-controllable growth of ultrathin 2D magnetic  $\text{FeTe}$  crystals. *Nature Communications*, **2020**, 11 (1): 3729.
- [78] Zhao L L, Li Y Z, Zhao X M, et al. Dirac-cone-like electronic states on nematic antiferromagnetic  $\text{FeSe}$  and  $\text{FeTe}$ . *Journal of Physics: Condensed Matter*, **2022**, 34 (32): 325801.
- [79] Liu L, Kankam I, Zhuang H L. Single-layer antiferromagnetic semiconductor  $\text{CoS}_2$  with pentagonal structure. *Physical Review B*, **2018**, 98 (20): 205425.
- [80] Teruya A, Suzuki F, Aoki D, et al. Fermi surface and magnetic properties in ferromagnet  $\text{CoS}_2$  and paramagnet  $\text{CoSe}_2$  with the pyrite-type cubic structure. *Journal of Physics: Conference Series*, **2017**, 807: 012001.
- [81] Wang X, Zhou Z, Zhang P, et al. Thickness-controlled synthesis of  $\text{CoX}_2$  ( $X = \text{S}, \text{Se}, \text{and Te}$ ) single crystalline 2D layers with linear magnetoresistance and high conductivity. *Chemistry of Materials*, **2020**, 32: 2321–2329.
- [82] Liu H F, Wong S L, Chi D Z. CVD growth of  $\text{MoS}_2$ -based two-dimensional materials. *Chemical Vapor Deposition*, **2015**, 21 (10): 241–259.
- [83] Liu S, Yuan X, Zou Y, et al. Wafer-scale two-dimensional ferromagnetic  $\text{Fe}_3\text{GeTe}_2$  thin films grown by molecular beam epitaxy. *npj 2D Materials and Applications*, **2017**, 1: 30.
- [84] Gong Y, Guo J, Li J, et al. Experimental realization of an intrinsic magnetic topological insulator. *Chinese Physics Letters*, **2019**, 36: 076801.
- [85] Wu W, Combs N G, Stemmer S. Molecular beam epitaxy of phase-pure antiperovskite  $\text{Sr}_3\text{SnO}$  thin films. *Applied Physics Letters*, **2021**, 119: 161903.
- [86] Wang J, Powers W, Zhang Z, et al. Observation of coexisting weak localization and superconducting fluctuations in strained  $\text{Sn}_{1-x}\text{In}_x\text{Te}$  thin films. *Nano Letters*, **2022**, 22: 792–800.
- [87] Ren Z, Li H, Sharma S, et al. Plethora of tunable Weyl fermions in kagome magnet  $\text{Fe}_3\text{Sn}_2$  thin films. *npj Quantum Materials*, **2022**, 7: 109.
- [88] Deng Y, Yu Y, Song Y, et al. Gate-tunable room-temperature ferromagnetism in two-dimensional  $\text{Fe}_3\text{GeTe}_2$ . *Nature*, **2018**, 563: 94–99.
- [89] Gong C, Li L, Li Z, et al. Discovery of intrinsic ferromagnetism in two-dimensional van der Waals crystals. *Nature*, **2017**, 546: 265–269.
- [90] Huang Y, Pan Y H, Yang R, et al. Universal mechanical exfoliation of large-area 2D crystals. *Nature Communications*, **2020**, 11: 2453.
- [91] Lee J U, Lee S, Ryoo J H, et al. Ising-type magnetic ordering in atomically thin  $\text{FePS}_3$ . *Nano Letters*, **2016**, 16: 7433–7438.
- [92] Wang X, Du K, Fredrik Liu Y Y, et al. Raman spectroscopy of atomically thin two-dimensional magnetic iron phosphorus trisulfide ( $\text{FePS}_3$ ) crystals. *2D Materials*, **2016**, 3: 031009.
- [93] Du K Z, Wang X Z, Liu Y, et al. Weak van der Waals stacking, wide-range band gap, and Raman study on ultrathin layers of metal phosphorus trichalcogenides. *ACS Nano*, **2016**, 10: 1738–1743.
- [94] Lee S, Choi K Y, Lee S, et al. Tunneling transport of mono- and few-layers magnetic van der Waals  $\text{MnPS}_3$ . *APL Materials*, **2016**, 4: 086108.
- [95] Wang X, Cao J, Lu Z, et al. Spin-induced linear polarization of photoluminescence in antiferromagnetic van der Waals crystals. *Nature Materials*, **2021**, 20: 964–970.
- [96] Kuo C T, Neumann M, Balamurugan K, et al. Exfoliation and Raman spectroscopic fingerprint of few-layer  $\text{NiPS}_3$  van der Waals crystals. *Scientific Reports*, **2016**, 6: 20904.
- [97] Hossain M, Qin B, Li B, et al. Synthesis, characterization, properties and applications of two-dimensional magnetic materials. *Nano Today*, **2022**, 42: 101338.
- [98] Nicolosi V, Chhowalla M, Kanatzidis M G, et al. Liquid exfoliation of layered materials. *Science*, **2013**, 340: 1226419.
- [99] Shioyai J, Ito Y, Mitsuhashi T, et al. Electric-field-induced superconductivity in electrochemically etched ultrathin  $\text{FeSe}$  films on  $\text{SrTiO}_3$  and  $\text{MgO}$ . *Nature Physics*, **2016**, 12: 42–46.
- [100] Chauhan P, Patel A B, Solanki G K, et al. Flexible self-powered electrochemical photodetector functionalized by multilayered tantalum diselenide nanocrystals. *Advanced Optical Materials*, **2021**, 9: 2100993.
- [101] Hui Z, Wang Y, Shen N, et al. Few-layer  $\text{ZrTe}_3$  nanosheets for ultrashort pulse mode-locked laser in 1.55  $\mu\text{m}$  region. *Optical Materials*, **2022**, 123: 111939.
- [102] Kong D, Randel J C, Peng H, et al. Topological insulator nanowires and nanoribbons. *Nano Letters*, **2010**, 10: 329–333.
- [103] Sobota J A, He Y, Shen Z X. Angle-resolved photoemission studies of quantum materials. *Reviews of Modern Physics*, **2021**, 93: 025006.
- [104] Shen Z, Zhu X D, Ullah R R, et al. Anomalous depinning of magnetic domain walls within the ferromagnetic phase of the Weyl semimetal  $\text{Co}_3\text{Sn}_2\text{S}_2$ . *Journal of Physics: Condensed Matter*, **2023**, 35: 045802.
- [105] Wang Q, Xu Y, Lou R, et al. Large intrinsic anomalous Hall effect in half-metallic ferromagnet  $\text{Co}_3\text{Sn}_2\text{S}_2$  with magnetic Weyl fermions. *Nature Communications*, **2018**, 9: 3681.
- [106] Belopolski I, Cochran T A, Liu X, et al. Signatures of Weyl fermion annihilation in a correlated kagome magnet. *Physical Review Letters*, **2021**, 127: 256403.
- [107] Cheng W, Wan B, Shen J, et al. Quasi-two-dimensional topological  $\text{Co}_3\text{Sn}_2\text{S}_2$  composite toward high rate sodium ion storage. *Chemical Engineering Journal*, **2022**, 443: 136420.
- [108] Fang Y, Pan J, Zhang D, et al. Discovery of superconductivity in 2M  $\text{WS}_2$  with possible topological surface states. *Advanced Materials*, **2019**, 31: 1901942.
- [109] Frolov S M, Manfra M J, Sau J D. Topological superconductivity in hybrid devices. *Nature Physics*, **2020**, 16: 718–724.
- [110] Shwetha G, Chandra S, Chandra Shekar N V, et al. Existence of spin-polarized Dirac cone in  $\text{Sc}_2\text{CrB}_6$ : A DFT study. *Physica B: Condensed Matter*, **2022**, 624: 413369.
- [111] Song W, Yan Z, Ban L, et al. Quantum conductivity in the topological surface state in the  $\text{SbV}_3\text{S}_5$  kagome lattice. *Physical Chemistry Chemical Physics*, **2022**, 24: 18983–18991.
- [112] Liu H, Zhong M, Ju M. Prediction of phonon-mediated superconductivity and topological surface states in  $\text{NbRu}_5\text{C}$ . *Physica B: Condensed Matter*, **2022**, 646: 414255.